AJBMS AFGHANISTAN Journal of Basic Medical Sciences
ISSN: 3005-6632

Afghanistan Journal of Basic Medical Sciences

2025 Jan 2(1):44-56.

ajbms.knu.edu.af

Investigating Aromadendrin Role as a Potential Inhibitor of Acyl-Homoserine Lactone Synthase through Molecular Docking and Dynamics

Shoib Omari, Abdul Musawer Bayan, *Zabihullah Adib Azizi, Rafiullah Shirzadi

Medical Sciences Research Center, Ghalib University, Kabul, Afghanistan

ARTICLE INFO

Type: Original Article

Received: 11 July, 2024

Accepted: 18 October, 2024

*Corresponding Author:

E-mail: dr.zabiullahadibazizi@ghalib.edu.af

To cite this article: Omari S, Bayan AM, Azizi ZA, Shirzadi R. Investigating Aromadendrin Role as a Potential Inhibitor of Acyl-Homoserine Lactone Synthase through Molecular Docking and Dynamics. Afghanistan Journal of Basic Medical Sciences. 2025 Jan 2(1):44-56.
https://doi.org/10.62134/khatamuni.60

ABSTRACT

Background: The widespread use of antibiotics to combat bacterial infections has led to the alarming rise of antibiotic resistance and the development of biofilms, both of which exacerbate disease severity and mortality rates. Biofilms, structured communities of bacteria, rely heavily on quorum sensing (QS)—a communication system that bacteria use to regulate collective behavior. This process is mediated by chemical signaling molecules known as autoinducers. Interrupting the production of these molecules, specifically by targeting key enzymes like acyl-homoserine lactone synthase (AHL synthase), could significantly boost antibiotic effectiveness and inhibit biofilm development. In this context, aromadendrin, a type of flavanonol in the flavonoid family, known for its wide-ranging medicinal benefits, is investigated for its capacity to inhibit AHL synthase activity.

Methods: To evaluate the interaction and binding affinity of aromadendrin with AHL synthase, molecular docking techniques were performed using AutoDock 4.2.2 software. Molecular dynamics (MD) simulations were employed utilizing the AMBER99SB force field and were executed within the GROMACS 2019.6 platform. The study performed in Ghalib Bioinformatics Center, Kabul. Afghianitan in 2024.

Results: The results from molecular docking and MD simulations demonstrated strong hydrogen bonding and van der Waals interactions with binding energy of -6.78 (KCal/mol) between aromadendrin and AHL synthase. These interactions highlight aromadendrin's potential as a promising inhibitor analog targeting AHL synthase.

Conclusion: By impeding bacterial communication pathways, aromadendrin can potentially diminish biofilm formation and enhance antibiotics' therapeutic impact, offering a novel and valuable approach to addressing antibiotic resistance and bacterial resilience.

Keywords: Acyl-homoserine lactones synthase, Aromadendrin, Molecular docking, Molecular dynamic simulation

Introduction

Bacteria use signaling molecules to sense their population density, modify gene expression, and respond to their environment, a process known as quorum sensing (QS) (1). QS functions as a bacterial communication system that coordinates cell behavior across a population in response to environmental changes through the creation and detection of

diffusible signal molecules (2). The core QS system consists of three main components: the signal synthase, the signal receptor, and the signal molecules (3). QS target genes include those that encode the proteins responsible for signal production, establishing an auto-inductive feedback loop to control signal molecule synthesis (4). This mechanism governs a range of bacterial activities, such as the production of virulence factors, secondary metabolites, biofilm formation, movement, and bioluminescence (5). Through complex regulatory networks, bacteria can activate specific genes based on their population size, facilitating synchronized group behavior (6). Different types of QS signal molecules are produced by bacteria. Gram-negative bacteria primarily produce N-acyl-homoserine lactones (AHLs), while Gram-positive bacteria use small linear peptides (e.g., ComX in Bacillus subtilis) or circular peptides (e.g., auto-inducing peptides AIP in *Staphylococcus aureus*) as signaling molecules that bind to receptors in a two-component system (7, 8).

Interest in quorum sensing mediated by acyl homoserine lactones (acyl-HSL) and the formation of bacterial biofilms has greatly increased in recent years (9). Quorum sensing controls the expression of virulence factors in various organisms, including *Pseudomonas aeruginosa*, a pathogen associated with cystic fibrosis (10). The formation of biofilms by *P. aeruginosa* poses a significant clinical challenge due to the high level of antibiotic resistance displayed by bacteria within these biofilms (11). The development of a mature P. aeruginosa biofilm depends on the production of the quorum sensing signal 3-oxo-dodecanoyl HSL (3OC12-HSL), demonstrating the importance of quorum sensing for biofilm development (12). Biofilm formation and quorum sensing have also been noted in Burkholderia cepacia complex (BCC) organisms, which can be problematic due to their potential high virulence and easy transmissibility among cystic fibrosis patients (13). Treating these infections is further complicated by the substantial antibiotic resistance exhibited by BCC organisms, which can be amplified when they form biofilms (13).

One of the major challenges of biofilms is their role in enhancing antibiotic resistance (14). Bacteria within biofilms show different growth rates and gene expression, resulting in increased resistance to antibiotics compared to free-floating (planktonic) bacteria (15). This resistance is multifactorial, involving physical barriers formed by the extracellular polymeric substance (EPS) matrix, modified microenvironments within the biofilm, and the presence of persistent cells that can endure antibiotic treatment (15). Biofilm formation is a complex process where microorganisms adhere to surfaces and create an EPS matrix (16). This matrix serves to protect the bacterial community and supports its growth and survival in diverse conditions (17). Biofilms are found in many environments, including medical devices, living tissues, water systems, and industrial surfaces (18). They are associated with numerous diseases, such as Cystic Fibrosis: Caused by *P. aeruginosa* (19), Otitis Media: Linked to *Haemophilus influenza* (20), Periodontitis: Involving *Porphyromonas gingivalis* and *Fusobacterium nucleatum* (21), Infective Endocarditis: Associated with *S. aureus*, viridans streptococci, and *Enterococcus faecalis* (22), Chronic Wounds: Often involving *P. aeruginosa* (23), Osteomyelitis: Also associated with *P. aeruginosa* (24), among others. These conditions underscore the critical role that biofilms play in chronic and persistent infections, making them difficult to treat (25).

Aromadendrin is a flavonoid compound or flavonoid glycoside, characterized by a flavonoid backbone connected to a sugar molecule, with a molecular formula of C15H14O7 (26). It belongs to the flavanol

category and is found in various plant species, particularly within the Cupressaceae and Lauraceae families (27). This compound has gained attention in both traditional medicine and scientific research due to its potential health-promoting properties. The main health benefits of aromadendrin include its powerful antioxidant properties, which help neutralize free radicals and protect cells from oxidative stress—a factor associated with aging and numerous diseases (28). Additionally, aromadendrin has notable anti-inflammatory effects, as it can reduce inflammation by inhibiting inflammatory pathways and regulating pro-inflammatory cytokines (26). It also supports cardiovascular health (29). Aromadendrin's antimicrobial properties make it effective against certain candidiasis (30). Moreover, it offers neuroprotective benefits, supporting cognitive function and possibly aiding in the prevention of neurodegenerative diseases like Alzheimer's and Parkinson's by protecting neuronal cells (31).

Molecular docking and MD simulations are computational methods in drug discovery and molecular biology, used to explore molecular interactions and dynamics (32). Molecular docking predicts the optimal orientation of a ligand when binding to a protein, allowing researchers to assess the interaction's strength and characteristics (32). In this study, these techniques were employed to investigate aromadendrin's inhibitory effects on AHLs synthase, aiming to interfere with quorum sensing.

Materials and Methods

Ligand and target Protein preparation

The ligands used in this study were obtained from the PubChem database with a CID of 122850 (32). The chemical structures were downloaded in SDF and converted to pdb format using Obabel software (33). The target protein structure was obtained from the Protein Data Bank (PDB) with PDB ID (1kzf) (34).

Molecular Docking

The interaction between Aromadendrin and AHLs synthase was investigated through a detailed molecular docking analysis, which was conducted at the Ghalib Bioinformatics Center, Kabul, Afghanistan in 2024, using the AutoDock 4.2.2 software package (35). To ensure a thorough exploration of the docking process, flexibility was maintained by allowing the torsion angles of the Aromadendrin molecules to rotate freely during the simulations. This approach enables the ligand to adopt various conformations, potentially enhancing the accuracy of the predicted binding interactions. The preparation of the AHLs synthase involved the addition of polar hydrogens, which was accomplished using the Hydrogen module in the AutoDock Tools (ADT). This step is crucial as it helps in accurately representing the protein's environment and facilitates better interaction modeling with the ligand. Following this preparation, the energy of the enzyme was minimized using GROMACS 2019.6 software, specifically employing the AMBER99SB force field (36). This energy minimization step ensures that the protein structure is in a stable conformation before docking, thus improving the reliability of the docking results. For the docking procedure, specific parameters were set that utilized an empirical free energy function alongside the Lamarckian genetic algorithm. The docking process was configured to allow for up to 25 million energy evaluations, which provides a comprehensive search of the conformational space. Additionally, a starting population of 300 individuals was randomly initialized to enhance the genetic algorithm's effectiveness in exploring potential binding configurations. This finely tuned grid allows for precise localization of binding sites on the AHLs

synthase. After conducting the docking simulations, the most favorable docked positions were selected based on the lowest binding energy, which was indicative of the most stable interactions within a highly clustered population of conformations. These selected positions, reflecting the most energetically favorable interactions, were subsequently utilized for further MD simulations, allowing for an in-depth analysis of the dynamic behavior and stability of the Aromadendrin-AHLs synthase complex over time.

Molecular Dynamics Simulation

MD simulations were performed using the GROMACS 2019.6 software package in conjunction with the AMBER99SB force field (36). To ensure the system was electrically neutral, chloride (Cl^-) and Sodium (Na^+) counter ions were incorporated to replace water molecules in the simulation setup. To obtain the necessary parameters for Aromadendrin, the ACPYPE tool, which is based on Python, was utilized (37). This tool facilitates the derivation of topological data for small molecules, enhancing the accuracy of the simulations. The initial phase of the simulation consisted of a 1 nanosecond (ns) run under NVT ensemble conditions, maintained at a temperature of 310 K and a pressure of 1 bar. Following this preliminary phase, a more extensive MD simulation lasting 300 ns was conducted, utilizing a time step of 2 femtoseconds (fs). Systematic analysis of the MD simulations involved generating graphical representations for key metrics such as root mean square deviation (RMSD), which measures the structural stability of the complex, and root mean square fluctuation (RMSF), which reflects the flexibility of specific residues. Additionally, the radius of gyration (Rg) was assessed to evaluate the compactness of the protein-ligand complex, while the solvent-accessible surface area (SASA) offered insights into the exposure of the complex to the solvent environment. Furthermore, the analysis included an examination of hydrogen bond interactions, which play a crucial role in stabilizing the binding of Aromadendrin to the 1KZF protein.

Results

Molecular docking

Table 1 details the binding energies and inhibition constants for the interaction between Aromadendrin and AHLs synthase. The results for the 1KZF-Aromadendrin system indicate a favorable binding energy, demonstrating a strong affinity between Aromadendrin and the enzyme which suggests that Aromadendrin has potential as an inhibitor of AHLs synthase. Molecular docking studies of the enzyme/ligand system show that Aromadendrin is correctly positioned within the active site of the 1KZF enzyme. Figure 1 illustrates the interactions between Aromadendrin and the key residues within the active site of 1KZF, which include Trp34, Tyr54, Tyr9, Leu12, Ser44, Asp48, Met42, Val67, Ser66, Arg68, and Arg100. The hydroxyl group of the ligand forms two hydrogen bonds with the carboxyl atoms of Ser44, a hydrogen bond with the carboxyl group of Glu43, and additional bonds with the carboxyl and amine group of Arg100. Based on these observations, the 1KZF-Aromadendrin complexes were selected for MD simulations to create more precise models of the ligand-receptor interactions under conditions that mimic the natural biological environment.

Table 1: The obtained docking results, binding energies and inhibition constants predicted by AutoDock program.

System	*ΔG binding (KCal/mol)*	*Ki (μM)*
AHLs synthase/Aromadendrin	-6.78	10.73

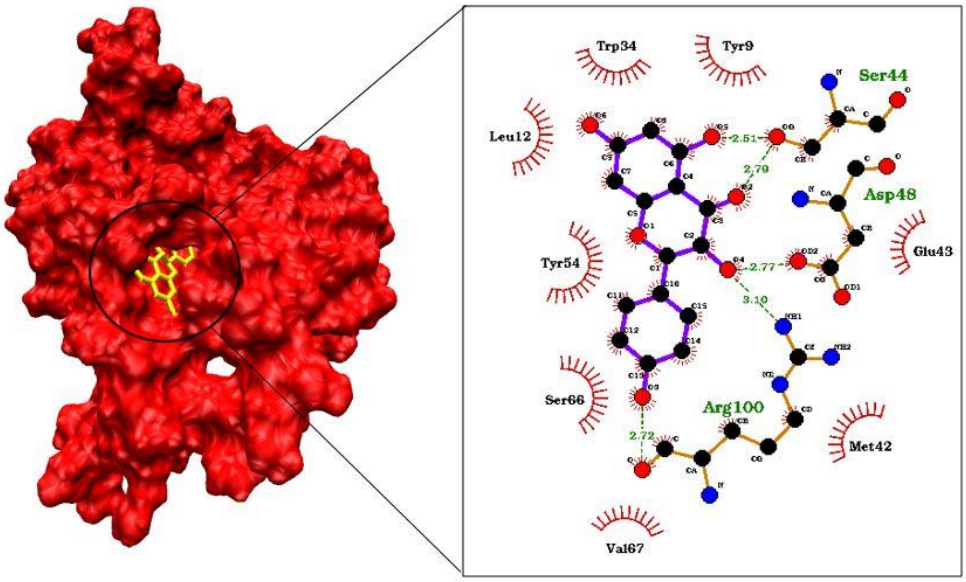

Figure 1: The best docking pose and molecular interactions of the Aromadendrin and the residues of the AHLs synthase. Figures provided by VMD1.9.3 and Ligplot+ programs.

Molecular dynamic simulation

RMSD

The RMSD analysis depicts the conformational changes within simulation time. Figure 2 shows the RMSD for the free enzyme and complex with aromadendrin. Importantly, the free AHLs synthase enzyme and Complex system, both stabilize around the 220 ns. The conformational instability of AHLs synthase is seen to be diminished in presence of aromadendrin, indicating that the complex form has more structural stability than AHLs synthase enzyme. Table 2 representing the average MD parameters for the last 30 ns, purposing that binding of aromadendrin to AHLs synthase causes the average RMSD to decline from 0.338±0.055 nm in its free state to 0.313±0.03 nm when complexed, indicating that the aromadendrin/1KZF complex has more structural stability than free 1kzf enzyme.

Table 2: The average and standard deviations of RMSD, Rg, RMSF and SASA for free and complex enzyme during the last 30ns.

System	*Mean RMSD (nm)*	*Mean Rg (nm)*	*Mean RMSF (nm)*	*Mean SASA (nm^2)*
1KZF	0.338±0.055	1. 766±0. 015	0. 129±0.079	117.231±2.635
1KZF/Aromadendrin	0.313±0.034	1. 709±0. 015	0.115±0. 048	112.691±2.892

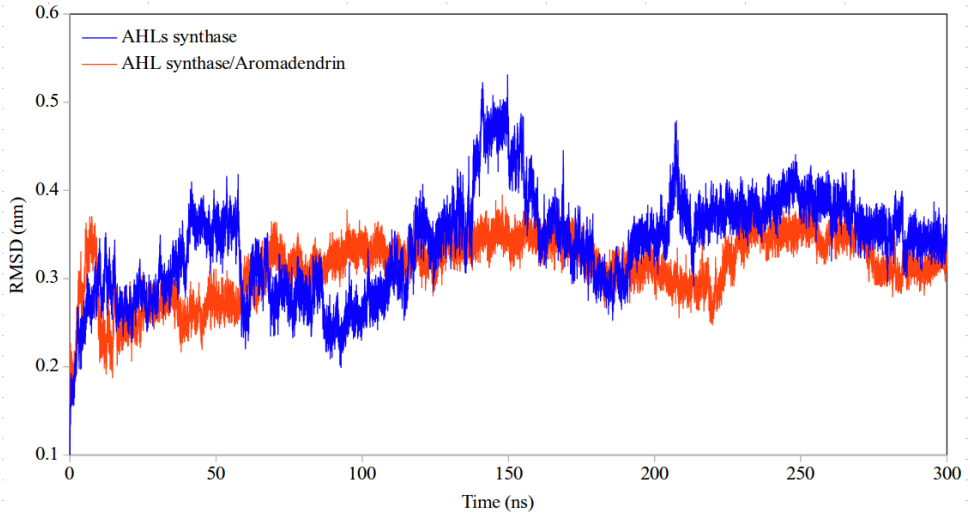

Figure 2: RMSD plots of free and bound enzyme as a function of time.

Analysis of the RMSF

The RMSF analysis, a computational method, explains the average deviation of residue. Figure 3 showing the RMSF values for both free enzyme and when it is complexed with aromadendrin. The residual fluctuations of AHLs synthase are seen to be diminished in conjugation with aromadendrin, indicating that the complex system has more structural stability than AHLs synthase enzyme. Additionally, the residues of AHLs synthase show a minimum RMSF value of 0.08 nm in all complexes, with a maximum reaching 0.78 nm. Importantly, as per the data in Table 2, the average RMSF value reduced when aromadendrin is present, from 0.129±0.079 nm in its free state to 0.115±0.048 nm in presence of aromadendrin, indicating that the AHLs synthase enzyme's complexed with aromadendrin has more structural stability, structural integrity and less conformational deviation of its residue than free form of AHL synthase.

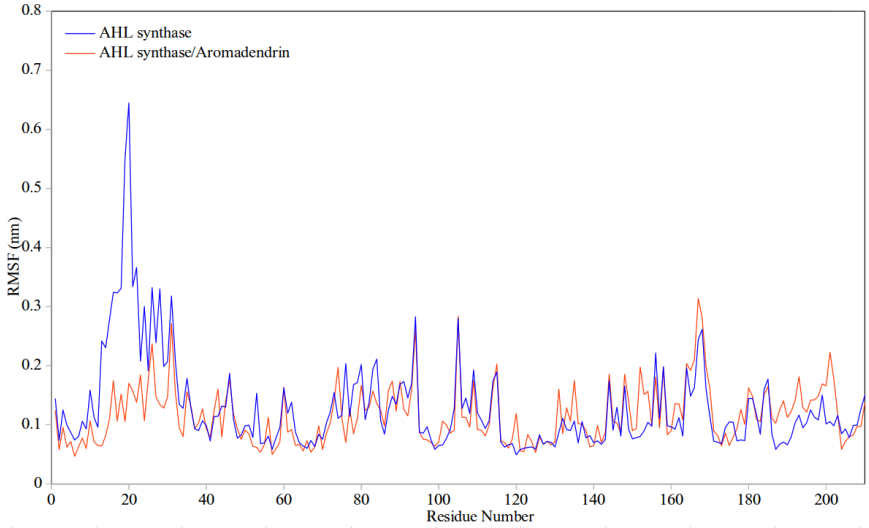

Figure 3: RMSF plots of free and bound enzyme.

Analysis of the radius of gyration (Rg)

The Rg analysis explaining the structural and conformational compactness of free and complex systems during simulation time. Figure 4 is displaying the Rg of the free 1KZF and 1KZF-Aromadendrin complexes.

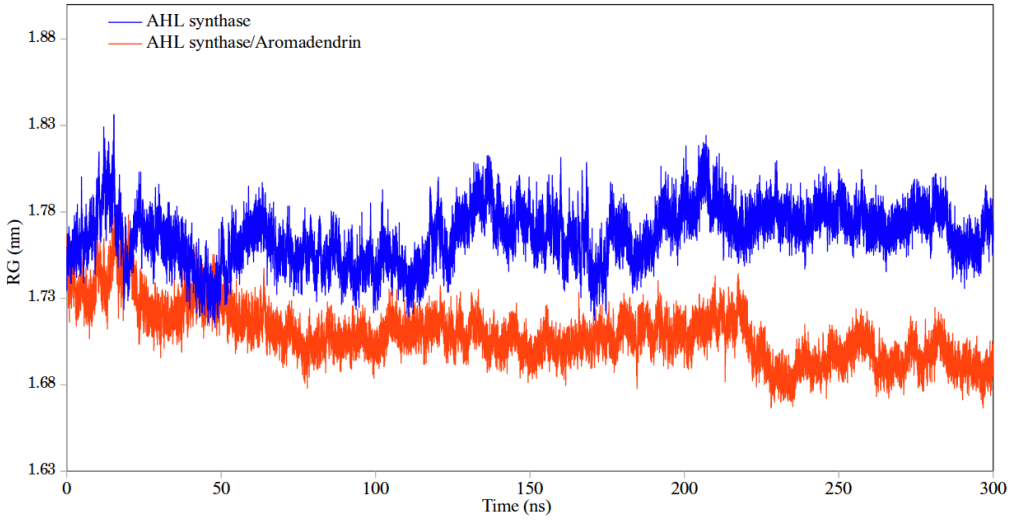

Figure 4: RG plots of free and bound enzyme as a function of time.

According to this plot, the AHLs synthase enzyme reaches equilibrium around 230 ns for free and complexed systems. The 3rd structure of 1KZF undergoes compression due to binding of aromadendrin, a changed from 1.83 to 1.68 nm in whole 300 ns simulation time, comparing the graph generated in RG of free and complex system respectively. In Table 2, Rg value throughout decreases from 1.766±0.015 to 1.709±0.015 in presence of aromadendrin respectively. This major changes in the average Rg of AHLs synthase in presence of aromadendrin binding offering that the enzyme's structure is highly condensed and its structural compactness is enhanced when aromadendrin attach to 1KZF.

Analysis of the SASA

SASA analysis allows us to understand the surface area of a biomolecule that is accessible to a solvent during the simulation time. Figure 5 represents SASA plot for free and complex form systems. According to this plot, the average SASA for the enzyme has diminished, in the presence of aromadendrin because aromadendrin replaces the previous solvent that existed and is contacted in the active site of AHLs synthase. The average SASA value show decreases when aromadendrin binds to AHLs synthase surface from 117.231±2.635 free form to 112.691±2.892 complex form respectively, transferring this idea that interaction of aromadendrin with AHLs synthase reduces the interaction of water molecules to the surface of the enzyme (Table 2). In addition, a decrease in the SASA average is also due to an increase in structural compactness (Rg). As the structural compactness of the enzyme is enhanced in the presence of aromadendrin, the surface area of the enzyme is shortened for accessible solvent.

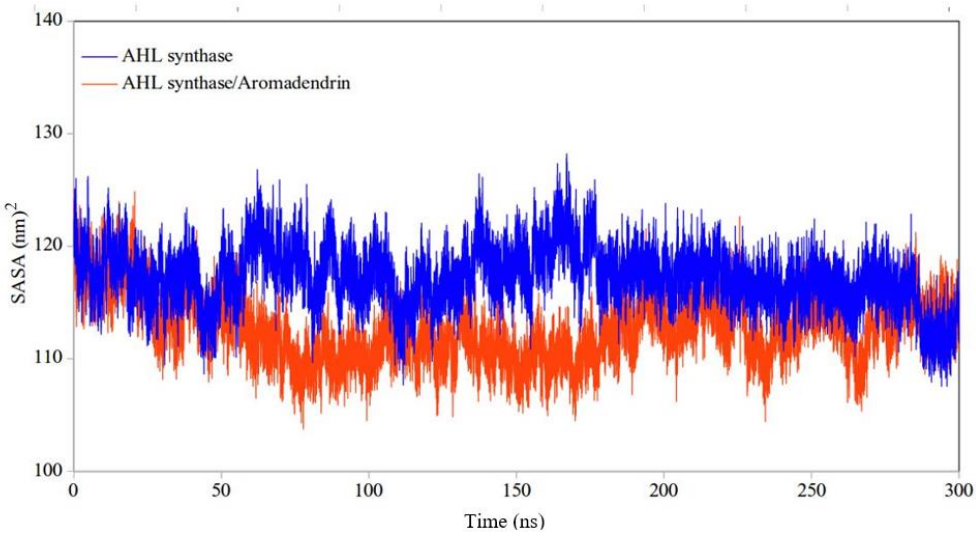

Figure 5: SASA plots of free and bound enzyme as a function of time.

Snapshots analysis

To examine the dynamic interaction between aromadendrin and the AHLs synthase enzyme, a snapshot analysis was conducted over a 300 ns simulation. This analysis captured positional changes of the ligand at 60 ns intervals, offering a detailed view of its binding behavior. As shown in Figure 6, Aromadendrin demonstrated less localization within the active site, remaining firmly stable without migrating or translocating to other regions of the enzyme surface except for 0 ns and 300 ns. Interestingly, while the ligand's position remained stable in a while, Aromadendrin displayed adaptive conformational changes to optimize its interactions. These adjustments facilitated the maintenance of hydrogen bonds with key amino acid residues in AHLs synthase, highlighting its strong binding affinity and flexibility.

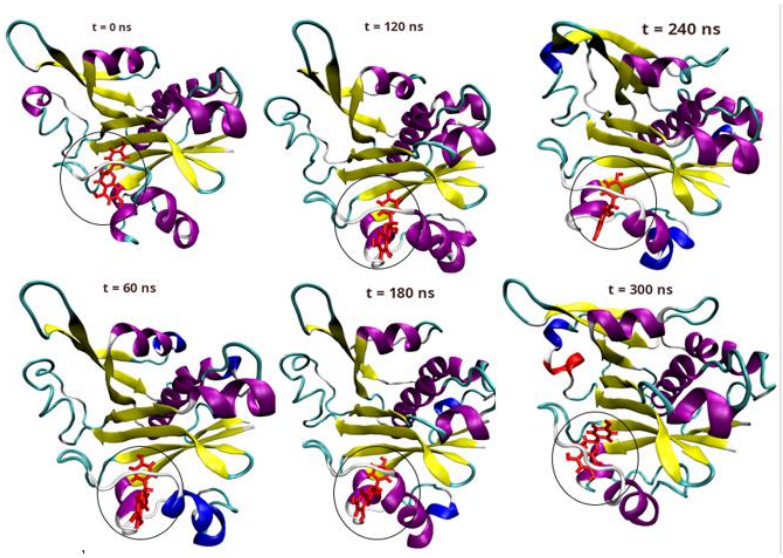

Figure 6: Snapshots plots of the AHLs synthase-Aromadendrin complex generated by VMD software.

Analysis of Hydrogen bonds

In MD simulations and docking study, investigating the H-bond analysis is essential for understanding molecular interactions, mainly the hydrogen interaction of Enzyme/Ligand, Enzyme/Enzyme and Enzyme/solvent. Figure 7 presents the hydrogen bonds between aromadendrin and the AHLs synthase. Maximum number of hydrogen bond generated between aromadendrin and AHL synthase were 5, in which implying the structural stability complexes. Figures 8 and 9 exhibiting the hydrogen bonding of Enzyme-Enzyme and Enzyme-Solvent for both the free and complex system during the simulation. According to plot 8, binding of aromadendrin to Enzyme lead to a mild elevation in Enzyme/Enzyme H-bond in graphic diagram, that is due to maintaining H-bond between complexes as interactions formed. Moreover, the binding of aromadendrin triggered to decrease the Enzyme-solvent H-bond that is due to replacement of solvent H-bond to Ligand/Enzyme H-bond, exhibited in Plot 9. Table 3 displaying average H-bond count. This table stating the raised average of Enzyme/Enzyme H-bond from free state 159.834±7.922 nm to 165.294±6.863 bound state, whereas there's a reduction in Enzyme/Solvent H-bond in presence of aromadendrin, a shift from 439.339±13.916 free state to 421.380±14.975 complex form correspondingly. That is clear that by binding of aromadendrin to enzyme, the number of enzyme's hydrogen bond increases however in other site ligand replaced the enzyme\solvent hydrogen bonds which leads to decrease in average of enzyme\solvent h-bond. In addition, SASA analysis which its interpretation explained previously, also decreased in presence of aromadendrin verifying above statement, that aromadendrin leads to diminish in intermolecular interaction and solvent accessible surface area for enzyme.

Table 3: The average and standard deviations of intra molecular enzyme and enzyme-solvent hydrogen bonds during last 30 ns

System	*Enzyme-Enzyme*	*Enzyme-Solvent*
Free 1KZF	159. 834±7.922	439.339±13.916
1KZF/Aromadendrin	165.294±6.863	421.380±14.975

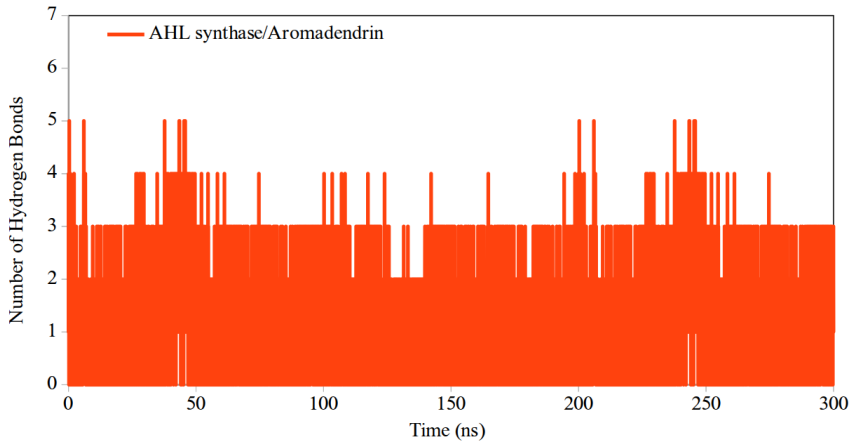

Figure 7: Time dependence of the number of hydrogen bonds between Aromadendrin and enzyme during the simulation time.

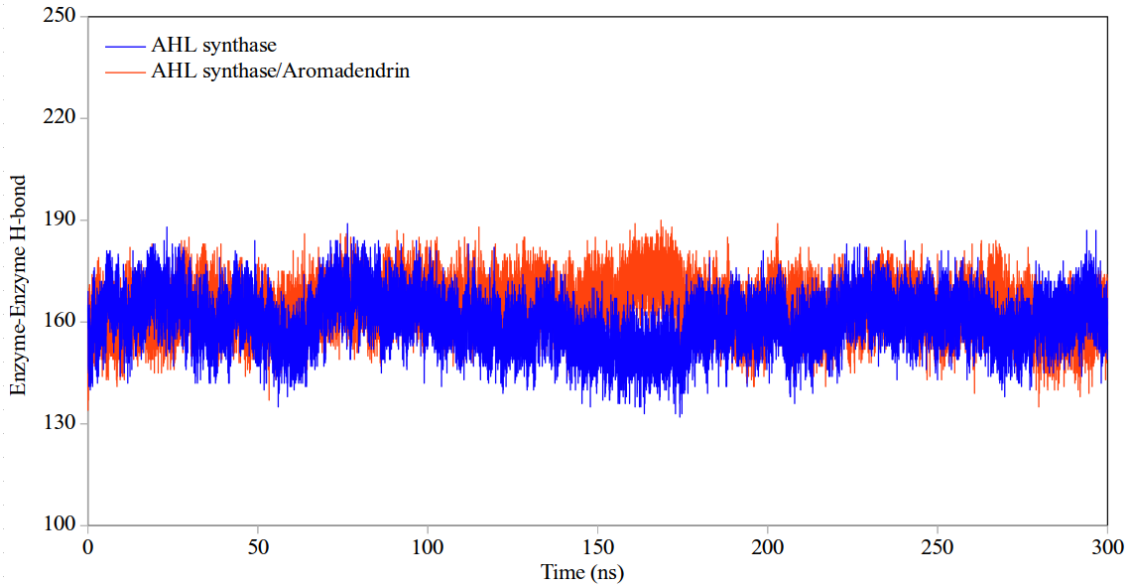

Figure 8: Enzyme - Enzyme hydrogen-bond plots of free and bound enzyme as a function of time.

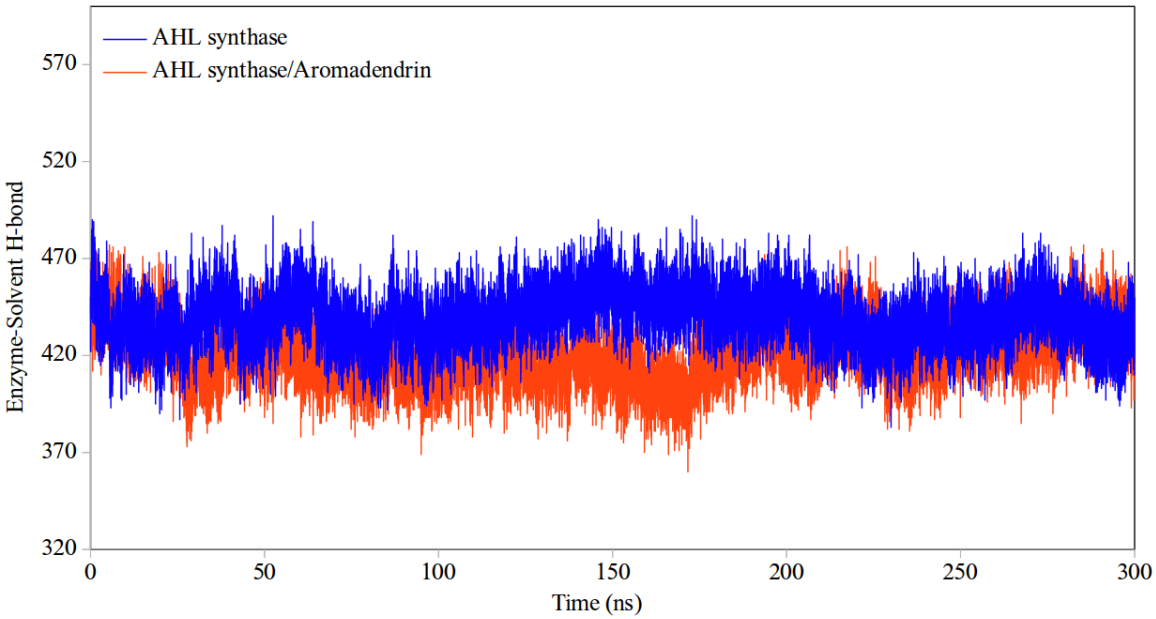

Figure 9: Enzyme-Solvent hydrogen bond plots of free and bound enzyme as a function of time.

Discussion

Utilizing both molecular docking and molecular dynamics simulations, this research explored the binding affinity, stability, and interaction mechanisms of taxifolin with AHL synthase, offering new insights into its inhibitory properties.

The MD findings indicated that taxifolin had a strong binding affinity for the active site of AHL synthase. This study underscores taxifolin's potential as an effective inhibitor of acyl-homoserine lactone (AHL) synthase. The results are consistent with earlier studies on flavonoids as quorum sensing inhibitors, like afzelechin, which showed comparable binding energies and interaction patterns (38, 39) . Nevertheless, taxifolin's greater structural stability offers a unique advantage,

suggesting its superior potential as an inhibitor.

Luteolin acts as a quorum sensing (QS) inhibitor owing to its strong affinity for the LasR regulator protein (40). Likewise, research conducted in 2019 found that plant-derived flavonoids such as quercetin and ellagitannins serve as anti-QS agents by targeting LuxI-type AHL synthases and LuxR-type receptor proteins (41). Additional investigations on inhibitors of AHL synthase from Acinetobacter baumannii (strain AYE) proposed compounds like Z815888654, Z2416029019, and Z3766992625 as promising inhibitors, along with Droperidol and Cipargamin, which also showed potential for inhibiting the enzyme's binding site (42, 43). Taxifolin's ability to hinder AHL synthase activity presents a significant opportunity for tackling bacterial resistance and infections associated with biofilms.

By disrupting quorum sensing, taxifolin could enhance the effectiveness of antibiotics and reduce biofilm development—an ongoing issue in medical settings. However, it is important to recognize the limitations of this study. The simulations were conducted under simplified in silico conditions, which might not adequately reflect the complexities of real biological environments. Future studies should aim to validate these results through in vitro and in vivo experiments to verify taxifolin's inhibitory effects and investigate its wider applications in fighting bacterial resistance.

Conclusion

Molecular docking and MD simulation applied to understand the inhibitory action of aromadendrin with AHLs synthase. Docking performed by 300 population size and simulations performed in 300 ns. Outputs from the molecular docking analysis unveiling favorable interactions of AHL synthase with aromadendrin in binding energy of -6.78 KCal/mol and constant inhibition of 10.73 µM. RMSD stating the stabilization of the AHL synthase in presence of aromadendrin. Rg plots showing the binding of aromadendrin to AHL synthase leading to increasing the structural compactness and condensation of AHL synthase 3rd structures. RMSF stating reduction in residue fluctuation of AHL synthase in presence of aromadendrin. SASA conferring a decline in solvent accessible surface area for AHL synthase in presence of aromadendrin. The hydrogen bonds generated between aromadendrin and the enzyme show the stability of complexes throughout the simulation time.

By analyzing the molecular interaction of aromadendrin with AHL synthase throughout computational technique, we find this that aromadendrin has potential inhibitory effect on AHL synthase, in which it can aid in designing new therapeutic agent against bacteria related with Qurom sensing and overall preventing chronic diseases by inhibiting biofilm formation.

Acknowledgments

This research was supported by resources supplied by the deputy of financial affairs of the Ghalib University, Kabul, Afghanistan. The authors would like to express their utmost gratitude to the Board of Directors of Ghalib University, Kabul, Afghanistan for support and motivations, especially Dr. M. I. Noori, Eng. A. Ahadi and Mr. N. A Nadeem. Special thanks to Mr. Mohammad Yousoof Saleh (Head of HR and financial affairs of Ghalib University) and his team, for assisting us in better performance of this study.

Conflict of interest

The authors declare that there is no conflict of interests.

References

1. Diggle SP, Crusz SA, Cámara M. Quorum sensing. Curr Biol. 2007;17(21):R907-R10.
2. Miller MB, Bassler BL. Quorum sensing in bacteria. Annu Rev Microbiol. 2001;55(1):165-99.
3. Hawver LA, Jung SA, Ng W-L. Specificity and complexity in bacterial quorum-sensing systems. FEMS Microbiol Rev. 2016;40(5):738-52.
4. Williams P, Camara M, Hardman A, Swift S, Milton D, Hope VJ, et al. Quorum sensing and the population-dependent control of virulence. PPhilos Trans R Soc Lond B Biol Sci. 2000;355(1397):667-80.
5. Cvitkovitch DG, Li Y-H, Ellen RP. Quorum sensing and biofilm formation in Streptococcal infections. J Clin Invest. 2003;112(11):1626-32.
6. Popat R, Cornforth D, McNally L, Brown SP. Collective sensing and collective responses in quorum-sensing bacteria. J R Soc Interface. 2015;12(103):20140882.
7. TINAZ GB. Quorum sensing in gram-negative bacteria. Turk J Biol. 2003;27(2):85-93.
8. Bhatt VS. Quorum sensing mechanisms in gram positive bacteria. Implication of quorum sensing system in biofilm formation and virulence. Springer. 2018:297-311.
9. Whiteley M, Diggle SP, Greenberg EP. Progress in and promise of bacterial quorum sensing research. Nature. 2017;551(7680):313-20.
10. De Kievit T. Quorum sensing in *Pseudomonas aeruginosa* biofilms. Environ Microbiol. 2009;11(2):279-88.
11. Jakobsen TH, Bjarnsholt T, Jensen PØ, Givskov M, H∅ iby N. Targeting quorum sensing in Pseudomonas aeruginosa biofilms: current and emerging inhibitors. Future Microbiol. 2013;8(7):901-21.
12. Zhao Q, Yang XY, Li Y, Liu F, Cao XY, Jia ZH, et al. N-3-oxo-hexanoyl-homoserine lactone, a bacterial quorum sensing signal, enhances salt tolerance in Arabidopsis and wheat. Bot Stud. 2020;61:1-12.
13. Suppiger A, Schmid N, Aguilar C, Pessi G, Eberl L. Two quorum sensing systems control biofilm formation and virulence in members of the Burkholderia cepacia complex. Virulence. 2013;4(5):400-9.
14. Cepas V, López Y, Muñoz E, Rolo D, Ardanuy C, Martí S, et al. Relationship between biofilm formation and antimicrobial resistance in gram-negative bacteria. Microb Drug Resist. 2019;25(1):72-9.
15. Becker P, Hufnagle W, Peters G, Herrmann M. Detection of differential gene expression in biofilm-forming versus planktonic populations of Staphylococcus aureus using micro-representational-difference analysis. Appl Environ Microbiol. 2001;67(7):2958-65.
16. O'Toole G, Kaplan HB, Kolter R. Biofilm formation as microbial development. Annu Rev Microbiol. 2000;54(1):49-79.
17. Bjarnsholt T, Buhlin K, Dufrêne Y, Gomelsky M, Moroni A, Ramstedt M, et al. Biofilm formation–what we can learn from recent developments. J Intern Med. 2018; 284(4):332-345.
18. Sauer K, Stoodley P, Goeres DM, Hall-Stoodley L, Burmølle M, Stewart PS, et al. The biofilm life cycle: expanding the conceptual model of biofilm formation. Nat Rev Microbiol. 2022;20(10):608-20.
19. Moreau-Marquis S, Stanton BA, O'Toole GA. Pseudomonas aeruginosa biofilm formation in the cystic fibrosis airway. Pulm Pharmacol Ther. 2008;21(4):595-9.
20. Akyıldız I, Take G, Uygur K, Kızıl Y, Aydil U. Bacterial biofilm formation in the middle-ear mucosa of chronic otitis media patients. Indian J Otolaryngol Head Neck Surg. 2013;65:557-61.
21. Jaffar N, Miyazaki T, Maeda T. Biofilm formation of periodontal pathogens on hydroxyapatite surfaces: Implications for periodontium damage. J Biomed Mater Res A. 2016;104(11):2873-80.
22. Di Domenico EG, Rimoldi SG, Cavallo I, D'Agosto G, Trento E, Cagnoni G, et al. Microbial biofilm correlates with an increased antibiotic tolerance and poor therapeutic outcome in infective endocarditis. BMC Microbiol. 2019;19:1-10.
23. Clinton A, Carter T. Chronic wound biofilms: pathogenesis and potential therapies. Lab Med. 2015;46(4):277-84.

24. Brady RA, Leid JG, Calhoun JH, Costerton JW, Shirtliff ME. Osteomyelitis and the role of biofilms in chronic infection. FEMSIM. 2008;52(1):13-22.
25. Chen L, Wen Ym. The role of bacterial biofilm in persistent infections and control strategies. Int J Oral Sci. 2011;3(2):66-73.
26. Patel K, Patel DK. Biological Potential of Aromadendrin Against Human Disorders: Recent Development in Pharmacological Activities and Analytical Aspects. Pharmacol Res Mod Chin Med. 2024:100424.
27. Mottaghipisheh J, Iriti M. Sephadex® LH-20, Isolation, and purification of flavonoids from plant species: A comprehensive review. Molecules. 2020;25(18):4146.
28. Wang Y, Yu Z, Yu Q. In vitro and in silico therapeutic properties of Artepillin C and Aromadendrin as collagenase and elastase inhibitors and investigation of anti-ovarian cancer effects and antioxidant potential. J Indian Chem. Soc. 2024;101(11):101367.
29. Cui S, Cui Y, Li Y, Zhang Y, Wang H, Qin W, et al. Inhibition of cardiac hypertrophy by aromadendrin through down-regulating NFAT and MAPKs pathways. Biochem Biophys Res Commun. 2018;506(4):805-11.
30. Rajesh P, Samaga PV, Ravishankar Rai V, Lokanatha Rai K. In vitro biological activity of aromadendrin-4′-methyl ether isolated from root extract of Ventilago madraspatana Gaertn with relevance to anticandidal activity. Nat Prod Res. 2015;29(11):1042-5.
31. Lee HS, Kim EN, Jeong G-S. Aromadendrin protects neuronal cells from methamphetamine-induced neurotoxicity by regulating endoplasmic reticulum stress and PI3K/Akt/mTOR signaling pathway. Int J Mol Sci. 2021;22(5):2274.
32. Santos LH, Ferreira RS, Caffarena ER. Integrating molecular docking and molecular dynamics simulations. Methods Mol Biol. 2019:13-34.
33. O'Boyle NM, Banck M, James CA, Morley C, Vandermeersch T, Hutchison GR. Open Babel: An open chemical toolbox. J Cheminform. 2011;3:1-14.
34. Berman HM, Battistuz T, Bhat TN, Bluhm WF, Bourne PE, Burkhardt K, et al. The protein data bank. Acta Crystallogr D Biol Crystallogr. 2002;58(6):899-907.
35. Morris GM, Goodsell DS, Halliday RS, Huey R, Hart WE, Belew RK, et al. Automated docking using a Lamarckian genetic algorithm and an empirical binding free energy function. J Comput Chem. 1998;19(14):1639-62.
36. Van Der Spoel D, Lindahl E, Hess B, Groenhof G, Mark AE, Berendsen HJ. GROMACS: fast, flexible, and free. J Comput Chem. 2005;26(16):1701-18.
37. Sousa da Silva AW, Vranken WF. ACPYPE-Antechamber python parser interface. BMC Res Notes. 2012;5:1-8.
38. Paczkowski JE, Mukherjee S, McCready AR, Cong J-P, Aquino CJ, Kim H, et al. Flavonoids suppress Pseudomonas aeruginosa virulence through allosteric inhibition of quorum-sensing receptors. J Biol Chem. 2017;292(10):4064-76.
39. Haidari F, Ataye AW, Ahmadyar ME, Bayan AM. Integrating molecular docking and molecular dynamics simulation studies of afzelechin as a potential inhibitor of Acyl-homoserine lactones (AHLs) synthase. AJBMS. 2024;1(2):43-52.
40. Geng YF, Yang C, Zhang Y, Tao SN, Mei J, Zhang XC, et al. An innovative role for luteolin as a natural quorum sensing inhibitor in Pseudomonas aeruginosa. Life Sci. 2021;274:119325.
41. Deryabin D, Galadzhieva A, Kosyan D, Duskaev G. Plant-derived inhibitors of AHL-mediated quorum sensing in bacteria: Modes of action. Int J Mol Sci. 2019;20(22):5588.
42. Jha RK, Khan RJ, Singh E, Kumar A, Jain M, Muthukumaran J, et al. An extensive computational study to identify potential inhibitors of Acyl-homoserine-lactone synthase from Acinetobacter baumannii (strain AYE). J Mol Graph Model. 2022;114:108168.
43. Jha RK, Singh E, Khan RJ, Kumar A, Jain M, Muthukumaran J, et al. Droperidol as a potential inhibitor of acyl-homoserine lactone synthase from A. baumannii: insights from virtual screening, MD simulations and MM/PBSA calculations. Mol Divers. 2023;27(5):1979-99.